Enhanced dielectric properties of immiscible poly (vinylidene fluoride)/low density polyethylene blends by inducing multilayered and orientated structures

Xiang Lin [a], Lili Fan [a], Dongyun Ren [b], Zhiwei Jiao [b], Weiming Yang [b], Phil Coates [c]

[a] *Department of Polymer Science and Engineering, School of Chemistry and Biological Engineering, University of Science and Technology Beijing, 100083, Beijing, China*

[b] *College of Mechanical and Electrical Engineering, Beijing University of Chemical Technology, 100029, Beijing, China*

[c] *Interdisciplinary Research Centre in Polymer Engineering, School of Engineering, Design, and Technology, University of Bradford, Bradford BD7 1DP, West Yorkshire, United Kingdom*

*** *Corresponding to***: *1. Xiang Lin; xiang003.buct@163.com. Tel/Fax: +8610 6233 4516;*

2. ZhiWei Jiao; jiaozw@mail.buct.edu.cn. Tel/Fax: +8610 6443 4734.

Abstract:

In order to improve the frequency-dependent dielectric properties of the immiscible polymeric blends which were melt-compounded by composing poly (vinylidene fluoride) (PVDF) and low density polyethylene (LDPE), the layer multiplication and the solid phase orientation technologies were respectively adopted as two effective strategies to optimize the dispersion state and the orientation of internal microstructure, aiming at reducing physical porosity and improving the barrier performance as well as crystal phase of the polymer extrudates. Results comparison showed the dielectric properties were greatly dependent on the crystal type and the physical porosity density which were also emphasized as the interfacial effect in the previous work [*ref. 29: Lin X et al, J Appl Polym Sci 2015; 132(36), 42507*]. It was found that the multilayer-structure manipulation could substantially improve the dispersion state between the two immiscible components, enhance the mechanical performance and reduce the internal defects and increase the dielectric constant while keeping the dielectric loss stable. By uniaxial stretching the sample sheets at a rubber state temperature of *ca.* 10-20˚C below the melting point, crystal transformation was induced by increasing molecular chains orientation degree which was also contributed to the enhancement of the dielectric properties. These techniques implied the potential as a promising way for inducing functional structures of polymeric blends.

Keywords: Polymer blends; Dielectric properties; Multilayer structure; Solid phase orientation.

1 Introduction

Owing to the outstanding processability, excellent ductility and effective cost, flexible polymers with high dielectric constant (high-ε) are desirable in the development of new generation of energy conversion and pulse energy storage. In the search for such materials exhibiting good flexibility and high permittivity, poly (vinylidene fluoride) (PVDF) [1-2] which possesses a high-ε of *ca.* 8-10 at room temperature [3], presenting unique piezoelectric, pyroelectric, ferroelectric and electro-acoustic properties [4-5], are widely used as a polymeric dielectric material. These excellent properties of PVDF are dependent on the unique β-crystal phase, in which PVDF molecular chains are arranged with a zigzag (all-trans, TTT) conformation. The β-crystals of PVDF could be generally obtained by applying straining, quenching or polarizing under a high electric field. Other different crystal phases within PVDF matrix, including α, γ and δ phases which are largely dependent on the molecules packing morphology, were also found and well documented in literatures [6-7]. Coexisting of crystallized and amorphous phases was well proved for the so-called crystallized polymers, i.e., semicrystalline structure [8-9]. A strong molecular inter-atomic force is beneficial to mechanical strength, elastic modulus as well as wear-resistance. Semicrystalline polymers upon drawing tend to exhibit yielding behavior during which the crystallinity and the crystallization morphology play a crucial role. Major properties enhancement is found to occur with the semi-crystalline polymers by solid phase processing owing to the optimization of crystallization structure. In both melt processing and solid phase processing of polymers there is an increasing awareness and understanding of the complex interplay between material kinetics and process dynamics.

The requirement of high energy density of polymeric dielectrics, which was applied as the broadest possible for capacitors and insulators, was driven by the need of fast charging/discharging. The energy density Q was theoretically expressed by

$$Q = \frac{1}{2}\varepsilon\varepsilon_0 E^2 \qquad (1),$$

where E is the electric field between the electrodes, ε is the relative dielectric constant of dielectrics, and ε^0 is the dielectric constant of vacuum and equals 8.85×10^{-12} F/m. Thus, it is possible to improve the energy density by increasing dielectric constant ε withstanding a certain electric field E.

It is universally acknowledged that not only each component itself but also the process history strongly dominates the internal microstructure of cooled packing molecules as well as the final performance of polymer composited products [10-13], especially for the immiscible blend systems [14]. For miscible polymer blend systems, researchers found that the micro-layered structure could effectively enhance the dielectric performance, including dielectric constant, loss, strength and energy density. Dielectric performance of polymeric blends, such as PVDF/polycarbonate (PC) [15], linear low density polyethylene (LLDPE)/ethylene vinyl alcohol (EVOH) [16] and PC/Poly(vinylidene fluoride-cohexafluoropropylene) [17-19] were thoroughly studied by co-extruding multilayer structure, aiming to enhance the energy density for electronic and electrical power applications. Due to the well regular arrangement of the nano-inclusions and the amazing increase on the number of the layer, micro-layer co-extrusion obtained by layer multiplication technology becomes one of the popularly adopted methods in processing functional polymeric film or in molding containers [20]. Such layered structures are always followed by advantages of excellent barrier performance, effective cost and significant reduction of internal defects [20-24]. Different polymer melts can be co-extruded in manner of films which trigger the diffusion of gas and water molecules more difficult and practically reduce the consumption of high cost resin without losing the desired performance. A large number of the new generated interfaces can improve the ability of reducing defects between different phases, leading to improvements of interfacial

properties.

Highly imparted orientation of macromolecule chains can be obtained by solid phase processing which is performed at a rubber state temperature of 10-20˚C below the melting point T_m [25-27]. The reduction of the molecular mobility and the increase of molecular orientation were reported as the dominant contribution to the significant enhancement of single property or combinations of properties [28]. The crystallization morphology was largely reorganized after orientation and remained stable in final products. When such orientation technology comes to a composite system, the regular arrangement of the inclusions is helpful to reduce internal defects or even change the morphological structure, giving rise to a variation of bulk density and a loss of conformational entropy. Meanwhile, the increase of polymer melting point and super-cooling degree are going to be advantageous to the crystallization occurrence. As an effective way for self-reinforced polymers, Ward and Coates et al [27] explored the mechanism and the practical applications for various polymers with different draw parameters in the past studies. The drawing ratio, drawing speed and die temperature were emphasized as the critical factors affecting the morphology deformation and final performance of drawn products.

For the certain PVDF/LDPE blends, how to increase the dielectric constant but non essential to increase the breakdown strength or to decrease the dielectric loss became the motivation in this work. Immiscible polymeric blends PVDF/LDPE was melt compounded with a co-rotating twin-screw extruder (D=20 mm, L/D=25). The layer multiplication and the die drawing techniques were adopted for the optimization of distribution state and phase structure, aiming to improve the dielectric performance. The crystallization transformation behavior and the dispersion improvement were emphasized as the contribution to the improvement of dielectric properties. An even sea-island structure was obviously observed after structure optimization process.

2 Experimental

2.1 Materials

A commercial PVDF (FR901 supplied by 3F Co. Ltd, China) with a density of 1.78 $g \cdot cm^{-3}$ and a melt flow index of 26 $g \cdot (10\ min)^{-1}$ was melt-compounded with the LDPE (LD100BW, Sinopec) pellets with a density of 0.923 $g \cdot cm^{-3}$ and a melt flow index of 2.0 $g \cdot (10\ min)^{-1}$ for composite cooperation. Coupling agents such as maleic anhydride (MAH), dicumyl peroxyide (DCP), dispersant and compatibilizer such as styrene and solvents including dimethylformamide (DMF) and xylene were selected from domestic companies.

2.2 Sample preparation

Dried PVDF pellets and LDPE/MAH/DCP/styrene (mass ratio 91.7: 4.0: 0.3: 4.0 wt.%) were melt-blended through the Haake mixer at 180˚C for 15 min. Then the PVDF/LDPE-g-MAH blends were hot-compressed into plaques for further die drawing process. Based on the previous work [28-29], the certain blend with the composition ratio of PVDF/LDPE=3/7 (wt.%) was taken as example in the present research. In addition, blended sheets were hydro-extruded by a single screw extruder through a layer multiplier under melt condition with a thickness of *ca.* 0.65 mm and a layered-structure of 1, 9, 81 and 729 layers, respectively.

Fig. 1

Table 1

Three multilayer units were mounted in series between die and single-screw extruder in this work. The principle of one flow multilayer unit is schematically illustrated in fig. 1.The flowing melt was preliminarily divided into 3 equal melt flows after passing through the first-half unit along the width direction and then each melt flow was turned 90˚ along the spiral channel and simultaneously the melt was extended in the width direction in the second-half unit and then was divided by 3 again. Thus, the single layer structure was finally changed into 9-layer structure. By combining *N* flow

multiplier units in series, the layers can be increased exponentially as 9^N layers.

Melt-compounded blends with a series of mass composition ratios of PVDF were additionally prepared for the die drawing operation. The applied temperatures for die drawing are illustrated in table 1. The drawing speed v was controlled at 100 mm/min for all samples apart from the pure PVDF billets. This uniaxial die drawing was performed with a modified tensile apparatus, as schematically shown in fig. 2. Drawing ratio, which was used to measure the tensile strain in this experiment was controlled by a pair of steel-plaques with a certain thickness, was calculated by $\lambda=d_0/d$. Thickness of the drawn billets was largely determined by the thickness of plaques. For the isotropic billets, the λ=1. Thus, the mechanical performance, especially tensile ductility, was crucial for the successful operation of the die drawing process.

Fig. 2

2.3 Main characterizations

Measurements of the crystallization kinetics were performed from 50 to 220˚C at 10.0˚C·min^{-1} by using a differential scanning calorimeter (Shimadzu DSC-60, Japan) within nitrogen atmosphere. Rheological measurements were conducted by the rotational rheometry MCR 501 (Anton-Paar GmbH, Austria) in oscillatory mode with a frequency range of 0.1-100 rad·s^{-1} at 180˚C. The oscillation shear was controlled with 1.0% strain deformation within air environment utilizing a parallel plate fixture. The X-Ray Diffraction (XRD) analyses were carried out on the DMAXRB 12 KW diffractometer (Rigaku, Japan) with the K-ray of copper (Cu) with the wavelength of *ca.* 0.15406 nm. The measured 2θ range was 10-100˚ with a scanning interval of 0.02˚ and scanning rate of 10.0˚ min^{-1}. All the dielectric measurements were performed on the Agilent 4294A impedance analyzer (USA) at room temperature over the frequency range of 10^2–10^6 Hz.

3 Results and Discussion

3.1 Dielectric properties of PVDF/LDPE-g-MAH with multilayered structure

The frequency dependence of ε and tanδ of structured PVDF/LDPE-g-MAH blends are given in fig. 3. Fluctuation of the measured data at low frequency ($f < 10^3$ Hz) was caused by the noisy signals, which usually can be ignored in practical. However, significant enhancement of the ε is observed for the multilayered samples, especially for samples with 729 layers whose dielectric constant is equivalent to the pure PVDF (ε=*ca.* 8) as well as the pure LDPE (ε=*ca.* 2.2). The dielectric loss of PVDF is *ca.* 0.05，while it comes to < *ca.* 0.02 for LDPE. From the results comparison, we can found that the dielectric loss of the blends presents a low amplitude variation, but dielectric constant shows an exciting increase only by inducing multilayer structure. Thus, the layering technique is expected to provide an effective method to increase the dielectric constant. Not only for polymer blends or/and nanocomposites with good compatibility [30], but also for those immiscible blend systems.

With the introduction of the multilayered structure, the thickness of a single layer decreases sharply on microscopic scale, which improves the interphase strength between PVDF and LDPE. The density increase of internal structure, therefore, is helpful for the elimination of internal defects between neighboring layers though they are the same bulk materials. Enhanced interfacial compatibility effect contributes to the better interface polarization, i.e., dielectric performance in this work. With an increased interfaces inducing by smaller subdivisions, the interfaces (between PVDF and LDPE domains) prevented the charge species from passing from one phase to the next, i.e., micro-confinement [24]. Different from the regular barrier effect reported by Bare et al. [16，30], the increased interfaces in present work are extremely irregular and randomly distributed.

Most multi-structured polymer films, which are always co-extruded and applied in functional fields, are going to take the advantage of the barrier effect, accompanied by an improved energy storage performance. Between two neighbored layers, generally speaking, are two pure layers which are

individual and alternated. It is well known that introducing a component that presents a barrier to the propagation of the electrical breakdown channel can increase the dielectric strength of the material. For a certain polymer material, the capacitive energy density improves with increasing dielectric constant and/or breakdown strength. In our work, the extruded sheets are obtained with a relatively large thickness, resulting in difficulty to evaluate the dielectric strength. However, a relatively increased breakthrough could be probably obtained according to references [18, 19] which are attributed to the results from the barrier effect of the layers. Even such barrier effect can prolong the dielectric lifetime during breakdown progress [17, 30].

In our work, the increased layer numbers, e.g. 729 layers, caused a great number of subdivisions in extrusion flow during multi-layering, i.e. interdependent and better dispersion, abruptly increases the interface areas. Baer and Mackey also suggested that the enhancement of dielectric performance of polycarbonate/PVDF should be attributed to the charge migration, instead of dipole flipping, for the dielectric hysteresis in the multilayers after increasing layers number [15].

Fig. 3

Crystallization kinetics of the immiscible blends with the multilayered structure was also investigated by DSC. Samples of PVDF/LDPE-g-MAH (3/7 wt.%) were taken as an example for discussion. As shown in Fig. 4, the mixing samples implies the plaques with single layer which was gotten by conventional extrusion casting or hot compressing, but the multilayered ones are obtained by the co-extrusion with the help of melt multiplier. Small deviations of both the melting temperature (T_m, fig. 4a) and the crystallization temperature (T_c, fig. 4b) of the LDPE/PVDF blends with different layers are revealed. It indicates that the multilayer co-extrusion manipulation plays an insignificant role in the thermal properties of these immiscible blends even though the shear effect is still presented from the difference of T_m and T_c between mixing and layer samples. This multilayer co-extrusion is good at improving the dispersion state of the two polymer phases, leading a better

surface quality, phase continuity and processability, as shown in fig. 5. The homogenous degree of PVDF domains were treated as the factor for considering dispersion quality. A better dispersion state of PVDF within the immiscible LDPE was obtained in the multilayer co-extruded sheets (seen in the SEM figs. 5 a2, a3 and a4). Meanwhile, multilayered interface was obviously found in the sheets obtained by multilayer co-extrusion as shown in fig. 5b. The increased multiplier behaves a static mixer here, leading to a discontinuous dispersion of the low composition phase, i.e., PVDF. In addition, the rheological results also support this conclusion which the immiscibility behavior is clearly shown by shearing an initially phase-separated phase, as shown in fig. 6. The viscosity and damping factor are greatly dependent on the content of PVDF (or LDPE), especially at low shear rates. Phase separation phenomenon is remarkable and sensitive at low shear rate, which implies no chemical reaction at all during the melt compounding process. It can be found that for the sample of PVDF/LDPE-g-MAH (3/7 wt.%), the viscoelastic behavior is still determined by the LDPE whose viscosity decreased abruptly at low shear frequency. This indicates a similar processability between the pure LDPE and PVDF/LDPE-g-MAH (3/7 wt.%).

Fig. 4

Fig. 5

The multilayer structure, furthermore, is found to be crucial for the homogeneous dispersion of MAH as well as PVDF in the blends, which is contributive to the enhancement of the mechanical performance, as shown in table 2. The measured maximum tensile stress increases with the quantity of layers, but the elongation at break decreases simultaneously. The abrupt increase of interface area should be responsible for the decrease of the break elongation, although small difference of the tensile strength among the samples with multilayer structure is revealed.

Fig. 6

Table 2

3.2 Effect of solid phase orientation on ε and tanδ of PVDF/LDPE-g-MAH

Effect of the solid phase orientation induced by die drawing is to produce a highly orientated structure, as shown in fig.7. Similar results were also reported in prior work when uniaxial drawing was applied on polypropylene/ multiwalled carbon nanotubes nanocomposites [28]. For crystallized polymer nanocomposites or miscible polymeric blends, it is well known that uniaxial or biaxial orientation progress will significantly change the dielectric performance, especially for miscible blends [31]. For an immiscible blend system, however, phase separation will be clearly shown after uniaxial deformation only if a fantastic compatible state is obtained.

In this work, frequency dependence of ε and tanδ of the uniaxial stretching billets was demonstrated in fig. 8. It can be seen that for pure LDPE, both ε and tanδ are independent on the frequency over the whole range of 10^3-10^6 Hz. However, the orientation degree, which is determined by the drawing ratio λ, i.e., 2.5 and 5 in present work, plays a significant role in the determination of dielectric performance. Compared with dielectric constant of pure LDPE at 10^3 Hz (ε=*ca.* 2.45), the ε of LDPE with λ=2.5 is *ca.* 5.8; otherwise, the ε of LDPE with λ=5 is *ca.* 4.2. The results are agreed with the XRD measurements, as shown in fig. 9. Apart from the increase of intensities, no new crystal phase is observed for pure LDPE (fig. 9a) which leads to a slight decrease on dielectric constant. The increased diffraction peak intensity implies that the degree of orientation enhancement. For PVDF, however, the β-crystal is found to be effective to enhance the dielectric performance (fig. 9b). Increase of the ε of the blends should be attributed to the formation of β and γ crystal of PVDF. In addition, the drawing speed is also positive to increase the ε of pure PVDF, causing which higher ε

(*ca.* 16 at 10^3 Hz) is observed for the samples drawn at 200 mm/s than those (ε=*ca.* 14 at 10^3 Hz) drawn at 100 mm/s. This indicates that both drawing rate and drawing ratio are helpful for promoting the formation of β and γ crystal.

Fig.7

Fig. 8

The drawing ratio, drawing speed and applied temperature are treated as the three dominant factors affecting the performance improvement of die drawing, especially for the immiscible blend systems. Drawing sample presented varied mechanical performance at varied temperatures, which is a critical determination to provide a success die drawing process. Each component of the blends will be extended along the drawing direction. As shown in fig. 9, it is clearly indicated that the effects of drawing ratio and speed on the arrangement and reformation of crystal grain. A higher drawing ratio consequently brings a higher orientation degree. An overview of the XRD patterns for the drawn samples is illustrated in fig. 10. Compared with the samples drawn at a higher λ or higher drawing speed (i.e., v=200 mm/min in this work), the diffraction peak intensity increases with the increase of λ or drawing speed, which implies an increased degree of crystal grain or molecular chains arranged along the drawing direction. Because this solid phase orientation process was operated under rubber-state and then cooled in ambient environment, so the induced transformation of crystalline structure was largely maintained in the final drawn billets. The improved dielectric properties are attributed to these regular arranged grains. Such results indicate the potential way in film or sheet casting field for inducing advanced structure with high dielectric performance.

Fig. 9

Fig. 10

4. Conclusions

The present work mainly focused on the two processing technologies- layer multiplication and solid phase orientation- for optimizing the frequency-dependent dielectric properties of the immiscible polymeric blends PVDF/LDPE. Results from the experimental analysis showed the dielectric properties were greatly dependent on the type of crystal phase (i.e., orientation) and the physical porosity density (i.e., layer numbers or phase dispersion and distribution). The multilayer-structure manipulation was found to substantially improve the dispersion state between the two immiscible components, enhance the mechanical performance and increasing the dielectric constant while keeping the dielectric loss stable. Solid phase orientation, achieved by uniaxial stretching the sample billets at a rubber state temperature of *ca.* 10-20˚C below the melting point which are extremely dependent on the mechanical performance, was beneficial to promote the β or γ crystal transformation by increasing molecular chains orientation degree, which was also contributed to the enhancement of the dielectric properties. These two structuring techniques demonstrated here has the potential for producing functional structures with enhanced properties for many of other applications.

Acknowledgements

The authors wish to thank the financial support of National Natural Science Foundation of China (NSFC51473018, 51503017), China Postdoctoral Science Foundation (2015M570928) and the Fundamental Research Funds for the Central Universities (FRF-TP-15-019A2).

Figure captions

Fig. 1 Flow principle of one multilayer unit.

Fig. 2 Schematically illustration of die drawing process: (a) drawing principle; (b) apparatus.

Fig. 3 Dielectric properties of the PVDF/LDPE-g-MAH blends: (a) dielectric constant; (b) loss tangent.

Fig. 4 Thermal analysis of the PVDF/LDPE blends from DSC: (a) endothermic flow; (b) exothermic flow.

Fig. 5 Morphologies of PVDF/LDPE-g-MAH blends with different layers: (a) dispersion state; (b) an overview of the cross-section of the sheets with 1- and 81-layers structure, respectively.

Fig. 6 Rheological properties of PVDF/LDPE-g-MAH blends: (a) damping factor; (b) complex viscosity.

Fig.7 Orientated structures of the uniaxial drawn samples.

Fig. 8 Effect of the drawing ratio on the dielectric properties: (a) dielectric constant; (b) loss tangent.

Fig. 9 Comparison of the XRD patterns of (a) LDPE and (b) PVDF at different drawing ratios and drawing speeds.

Fig. 10 An overview of the XRD patterns for PVDF/LDPE-g-MAH blends at different drawing ratios (solid ■ λ=2.5; open □ λ=5).

References

1. Xie YB, Du HX, Xia C. Porous poly (3, 4-ethylenedioxythiophene) nanoarray used for flexible

supercapacitor. Micropor Mesopor Mat 2015; 204: 163-172.

2. Huang H, Gan MY, Ma L, Yu L, Yang FF, Li YJ, Ge CQ. Fabrication of polyaniline/graphene/titania nanotube arrays nanocomposite and their application in supercapacitors. J Alloy Compd 2015; 630: 214-221.

3. Murugaraj P, Mainwaring D, Mora-Huertas N. Dielectric enhancement in polymer-nanoparticle composites through interphase polarizability. J Appl Phys 2005; 98: 054304-1-6.

4. Zhang QM, Li HF, Martin P, Xia F, Cheng ZY, Xu HS, Huang C. An all-organic composite actuator material with a high dielectric constant. Nature 2002; 419(6904): 284-287.

5. Li L, Wang SR, Hui D, Qiu J. Ordered multiphase polymer nanocomposites for high-performance solid-state supercapacitors. Compos Part B-Eng 2015; 71: 40-44.

6. Nan CW. Comment on “Effective dielectric function of a random medium”. Phys Rev B 2001; 63: 176201.

7. Dang ZM, Yuan JK, Zha JW, Zhou T, Li ST, Hu GH. Fundamentals, processes and applications of high-permittivity polymer-matrix composites. Prog Mater Sci 2012; 57: 660-723.

8. Zhang QM, Huang C. Enhanced dielectric and electromechanical responses in high dielectric constant all polymer percolative composites. Adv Funct Mater 2004; 14: 501-506.

9. Zhang QM, Li HF, Martin P, Feng X, Cheng ZY, Xu HS, Cheng H. An all-organic composite actuator material with a high dielectric constant. Nature 2002; 419(19): 284-287.

10. Brennecka GL, Ihlefeld JF, Maria JP, Tuttle BA, Clem PG. Processing technologies for high permittivity thin films in capacitor applications. J Am Ceram Soc 2010; 93: 3935-3954.

11. Tang CW, Li B, Sun LL, Lively B, Zhong WH. The effects of nanofillers, stretching and recrystallization on microstructure, phase transformation and dielectric properties in PVDF

nanocomposites. Eur Polym J 2012; 48: 1062-1072.

12. Gregorio R, Cestari M. Effect of crystallization temperature on the crystalline phase content and morphology of poly (vinylidene fluoride). J Polym Sci Part B: Pol Phys 1994; 32: 859-870.

13. Zhao J, Yin XQ, Shi JD, Dang ZM. Effect of the mixing on the dielectric constant of poly (vinylidene fluoride)/isotactic polypropylene blends. Sci Adv Mater 2013; 5: 1-7.

14. Xiong LZ, Yang WM, Li CJ, Zhou X, Jiao ZW. Plasticizer migration from micro-layered flexible poly (vinyl chloride) films prepared by multi-layer coextrusion technology. J Plast Film Sheet 2015; DOI: 10.1177/8756087915612884.

15. *Mackey M, Schuele DE, Zhu L, Flandin L, Wolak MA, Shirk JS, Hiltner A, Baer E. Reduction of Dielectric Hysteresis in Multilayered Films via Nanoconfinement. Macromolecules (2012); 45, 1954−1962.*

16. *Zhang GJ, Xu H, MacInnis K, Baer E. The structure-property relationships of LLDPE-EVOH blend films fabricated by multiplication extrusion. Polymer (2015); 57: 117-124.*

17. *Zhou Z, Mackey M, Carr J, Zhu L, Flandin L, Baer E. Fracture phenomena in micro- and nano-layered polycarbonate/poly(vinylidene fluoride-co-hexafluoropropylene) films under electric field for high energy density capacitors. J Appl Polym Sci (2014); 131(4), 39877.*

18. *Mackey M, Hiltner A, Baer E, Flandin L, Wolak M, Shirk JS. Enhanced breakdown strength of multilayered films fabricated by forced assembly microlayer coextrusion. J Phys D: Appl Phys (2009); 42, 175304.*

19. *Wolak MA, Pan MJ, Wan A, Shirk JS, Mackey M, Hiltner A, Baer E, Flandin L. Dielectric response of structured multilayered polymer films fabricated by forced assembly. Applied Physics Letters (2008); 92, 113301.*

20. Hirt SY, Hirt DE. Characterization of erucamide profiles in multilayer linear low-density

polyethylene and propylene-ethylene copolymer films using synchrotron-based Ft-Ir microspectroscopy. Appl Spectrosc 2002; 56: 205–211.

21. Lee PC, Dooley J, Robacki J, Jenkins S, Wrisley R. Improvements in flex oxygen barrier properties of polymeric films by microlayer coextrusion. J Plast Film Sheet 2014; 30: 234–247.

22. *Agoris DP, Vitellas I, Gefle OS, Lebedev SM, Pokholkov YP. The barrier effect in three-layer solid dielectrics in quasi-uniform electric field. J Phys D: Appl Phys (2001); 34, 3485-3491.*

23. *Vogelsang R, Farr T, Frohlich K. The effect of barriers on electrical tree propagation in composite insulation materials. IEEE Trans Dielectr Electr Insul (2006); 13, 373-382.*

24. *Lebedev SM, Gefle OS, Pokholkov YP. The barrier effect in dielectrics: the role of interfaces in the breakdown of inhomogeneous dielectrics. IEEE Trans Dielectr Electr Insul (2005); 12(3), 537555.*

25. Flory PJ. Thermodynamics of crystallization in high polymers and crystallization induced by stretching. J Phys Chem C 1947; 15: 397-408.

26. Coates PD, Caton-rose P, Ward IM, Thompson G. Process structuring of polymers by solid phase orientation processing. Sci China Chem 2013; 56: 1017-1028.

27. Ward IM, Coates PD, Dumoulin ME. Solid phase processing of polymers, PPS Series. Carl Hanser Verlag, ISBN 3-446-19622-6/ Hanser Gardner Publications, ISBN 1-56990-307-7, June 2000

28. Lin X, Tian JW, Hu PH, Ambardekar R, Thompson G, Dang ZM, Coates P. Improved dielectric performance of polypropylene/multiwalled carbon nanotube nanocomposites by solid-phase orientation. J Appl Polym Sci 2016; 133(3), 42893.

29. Lin X, Fan LL, Zhao J, Dang ZM, Ren DY. Effect of the compatibility on dielectric performance and breakdown strength of poly (vinylidene fluoride)/low density polyethylene blends. J Appl Polym

Sci 2015; 132(36), 42507

30. *Zhou Z, Mackey M, Carr J, Zhu L, Flandin L, Baer E. Multilayered Polycarbonate/Poly(vinylidene fluoride-cohexafluoropropylene) for High Energy Density Capacitors with Enhanced Lifetime. J Polym Sci Part B: Polym Phys (2012);50: 993–1003.*

31. Carr JM, Mackey M, Flandin L, Schuele D, Zhu L, Baer E. Effect of Biaxial Orientation on Dielectric and Breakdown Properties of Poly(ethylene terephthalate)/Poly(vinylidene fluoride-cotetrafluoroethylene) Multilayer Films. J Polym Sci Part B: Polym Phys (2013); 51: 882–896.

Figures

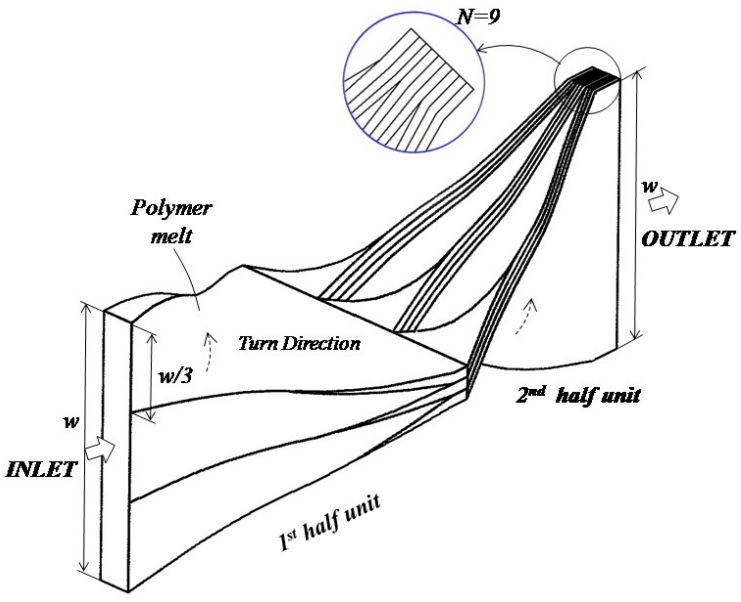

Fig. 1

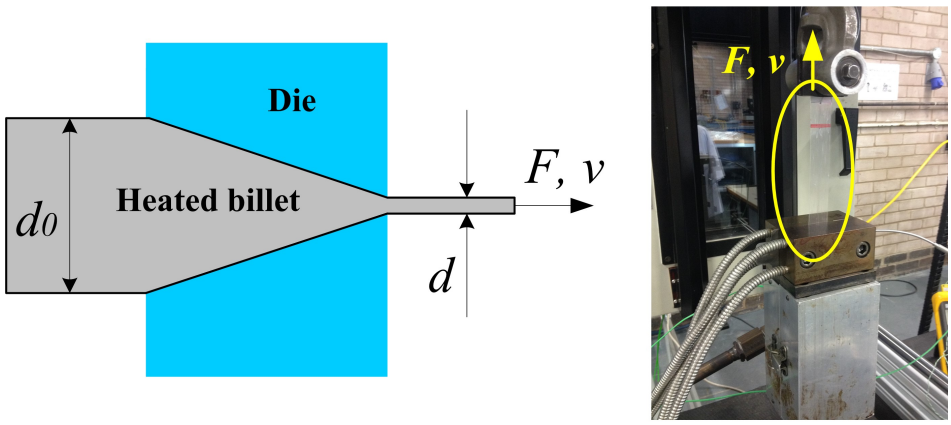
Die
Heated billet
d0
d
F, v
F, v

(a) (b)

Fig. 2

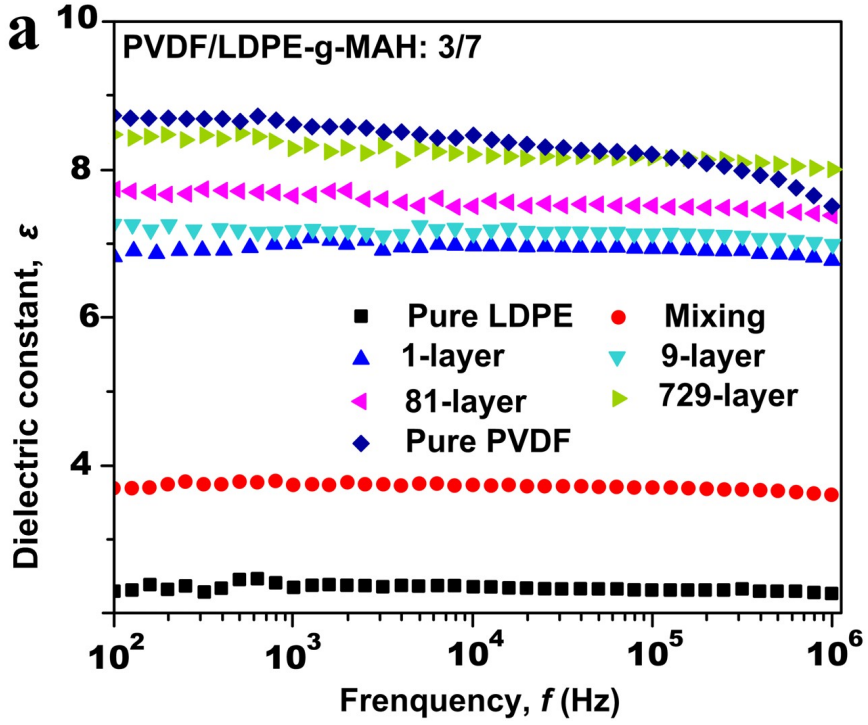
a
PVDF/LDPE-g-MAH: 3/7
Dielectric constant, ε
Frenquency, f (Hz)
Pure LDPE
Mixing
1-layer
9-layer
81-layer
729-layer
Pure PVDF

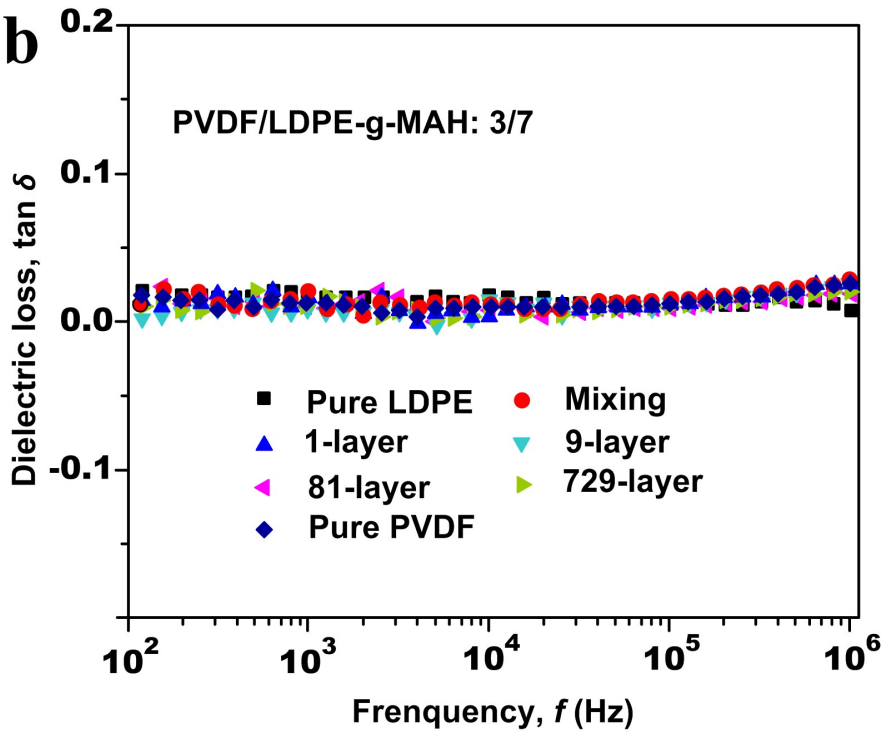
b
PVDF/LDPE-g-MAH: 3/7
Dielectric loss, tan δ
0.2
0.1
0.0
-0.1
Pure LDPE
1-layer
81-layer
Pure PVDF
Mixing
9-layer
729-layer
10^2
10^3
10^4
10^5
10^6
Frenquency, f (Hz)

Fig. 3

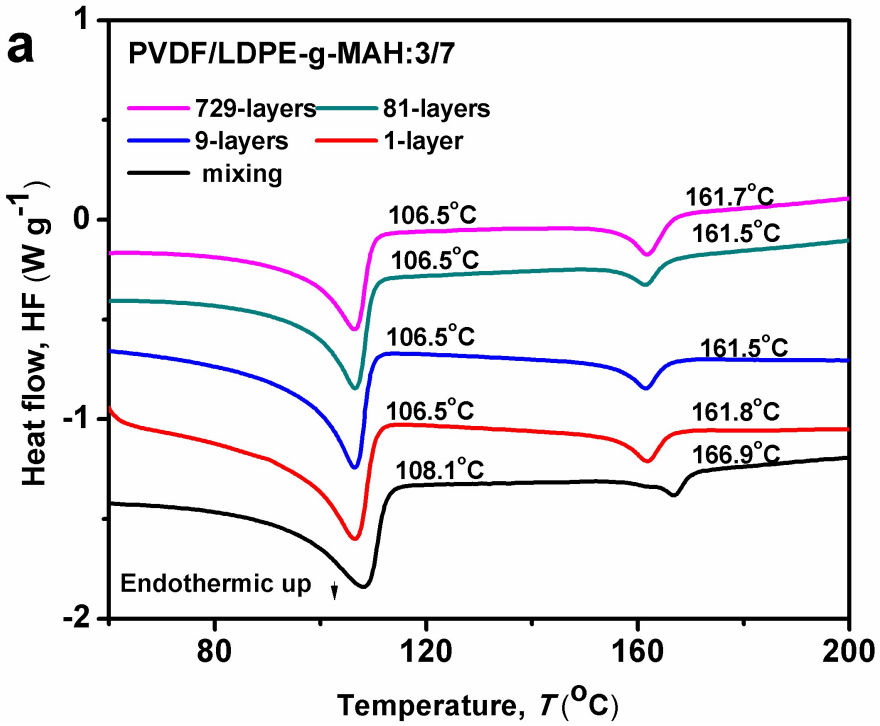
a
PVDF/LDPE-g-MAH:3/7
729-layers
81-layers
9-layers
1-layer
mixing
106.5°C
106.5°C
106.5°C
106.5°C
108.1°C
161.7°C
161.5°C
161.5°C
161.8°C
166.9°C
Endothermic up
Heat flow, HF (W g^-1)
1
0
-1
-2
80
120
160
200
Temperature, T (°C)

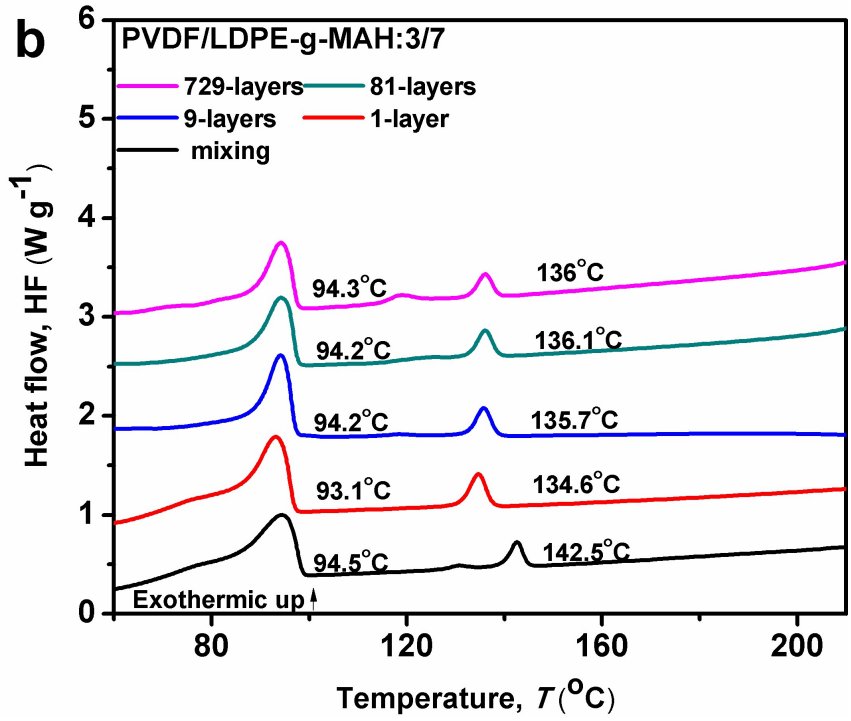
b
PVDF/LDPE-g-MAH:3/7
729-layers
81-layers
9-layers
1-layer
mixing
Heat flow, HF (W g-1)
94.3°C
136°C
94.2°C
136.1°C
94.2°C
135.7°C
93.1°C
134.6°C
94.5°C
142.5°C
Exothermic up
Temperature, T (°C)

Fig. 4

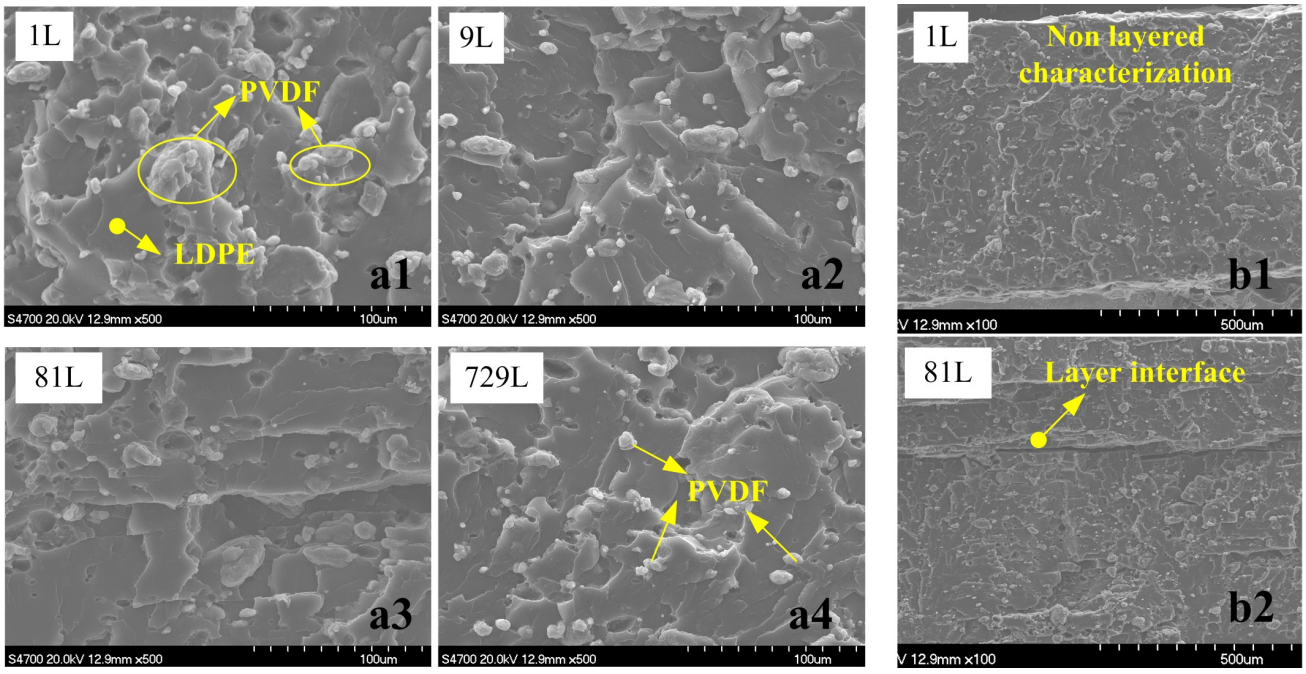
1L
PVDF
LDPE
a1
9L
a2
1L
Non layered characterization
b1
81L
a3
729L
PVDF
a4
81L
Layer interface
b2

Fig. 5

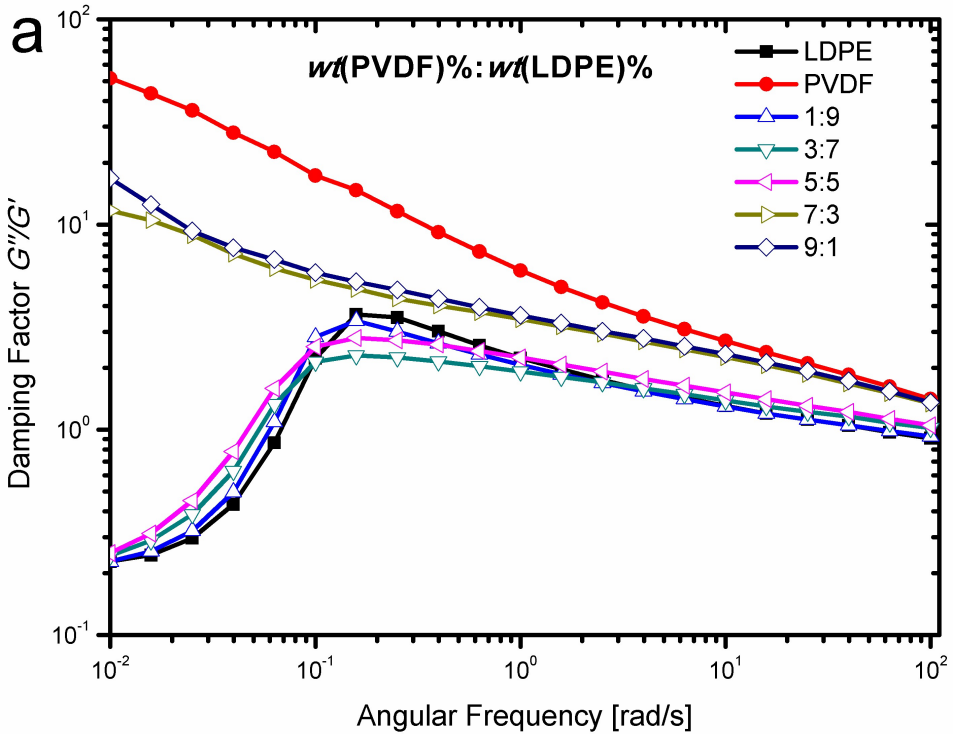
a
wt(PVDF)%:wt(LDPE)%
LDPE
PVDF
1:9
3:7
5:5
7:3
9:1
Damping Factor G''/G'
Angular Frequency [rad/s]

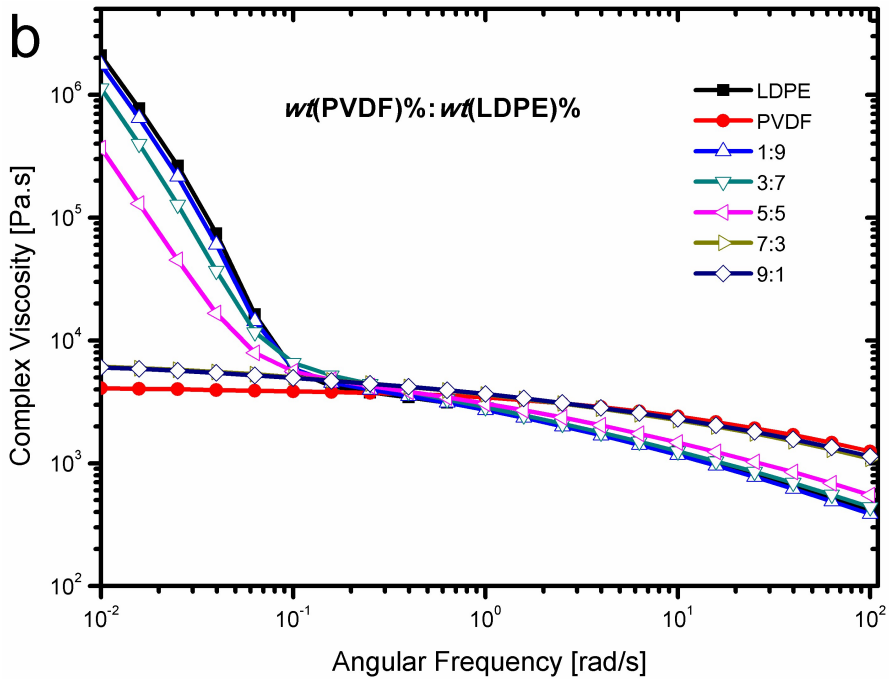
b
wt(PVDF)%:wt(LDPE)%
LDPE
PVDF
1:9
3:7
5:5
7:3
9:1
Complex Viscosity [Pa.s]
Angular Frequency [rad/s]

Fig. 6

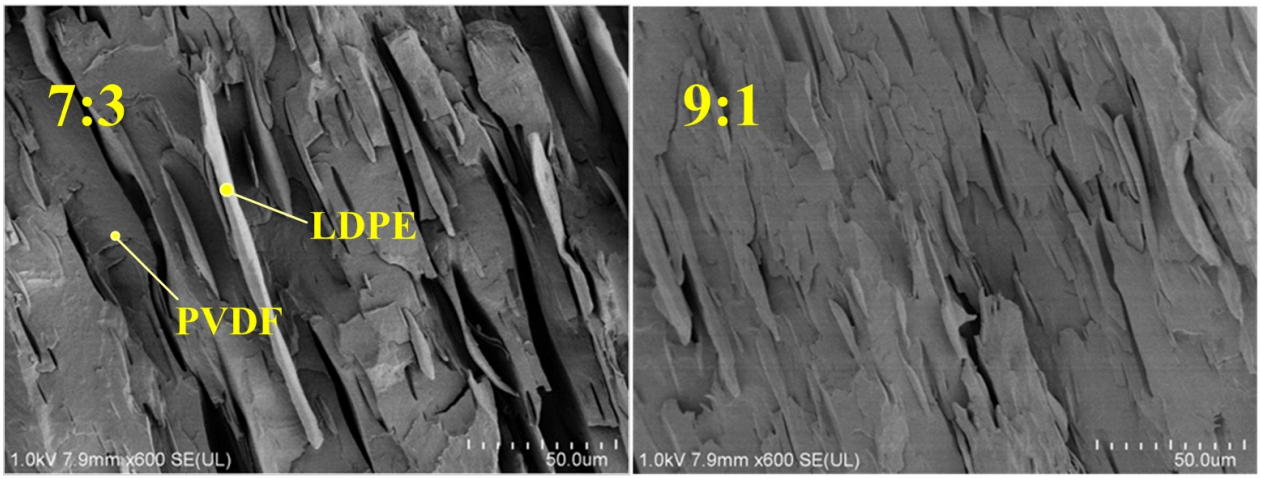
7:3
LDPE
PVDF
1.0kV 7.9mm x600 SE(UL)
50.0um
9:1
1.0kV 7.9mm x600 SE(UL)
50.0um

Fig. 7

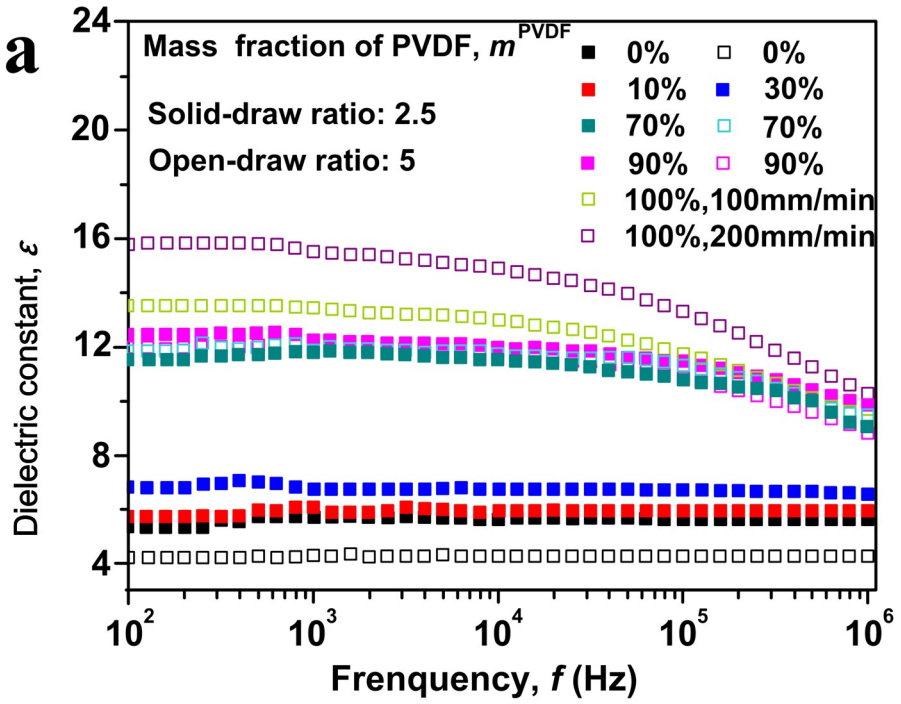
a
Mass fraction of PVDF, m^{PVDF}
Solid-draw ratio: 2.5
Open-draw ratio: 5
0%
0%
10%
30%
70%
70%
90%
90%
100%,100mm/min
100%,200mm/min
Dielectric constant, ε
Frenquency, f (Hz)
24
20
16
12
8
4
10^2
10^3
10^4
10^5
10^6

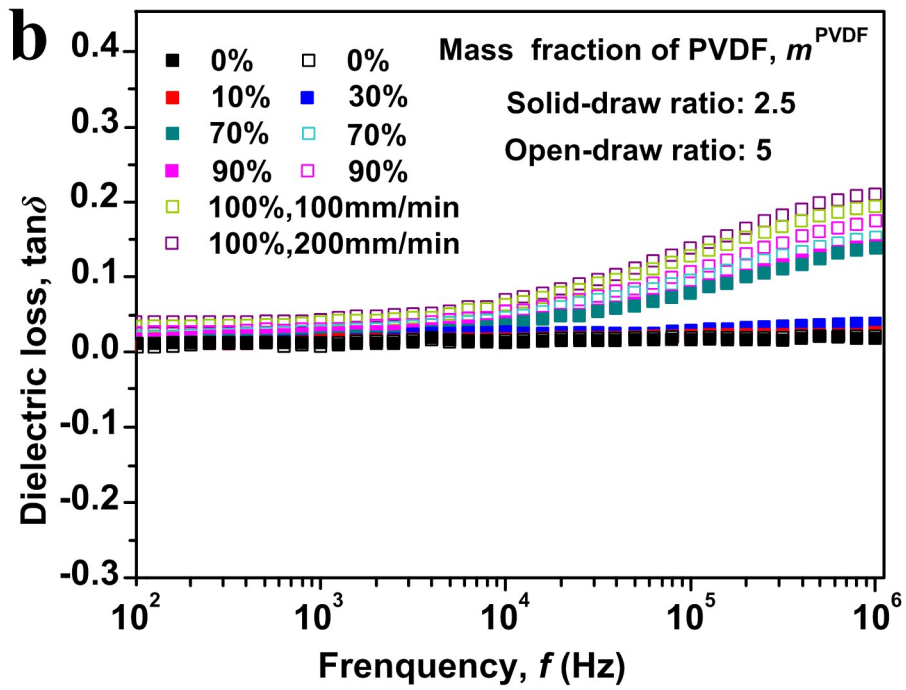
b
0.4
0.3
0.2
0.1
0.0
-0.1
-0.2
-0.3
Dielectric loss, tanδ
0%
10%
70%
90%
100%,100mm/min
100%,200mm/min
0%
30%
70%
90%
Mass fraction of PVDF, m^PVDF
Solid-draw ratio: 2.5
Open-draw ratio: 5
10^2
10^3
10^4
10^5
10^6
Frenquency, f (Hz)

Fig. 8

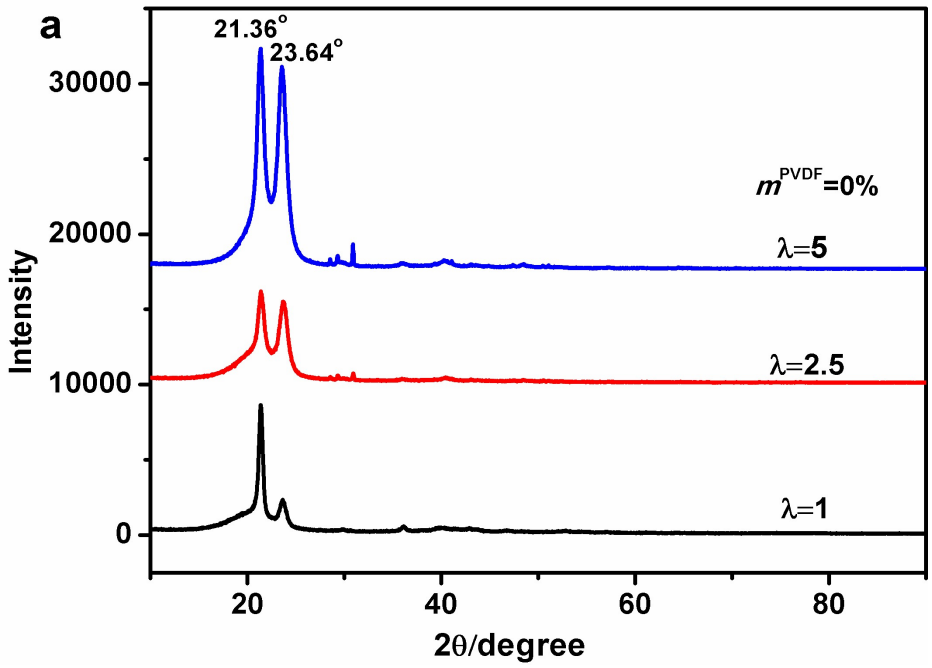
a
21.36°
23.64°
30000
20000
10000
0
Intensity
m^PVDF=0%
λ=5
λ=2.5
λ=1
20
40
60
80
2θ/degree

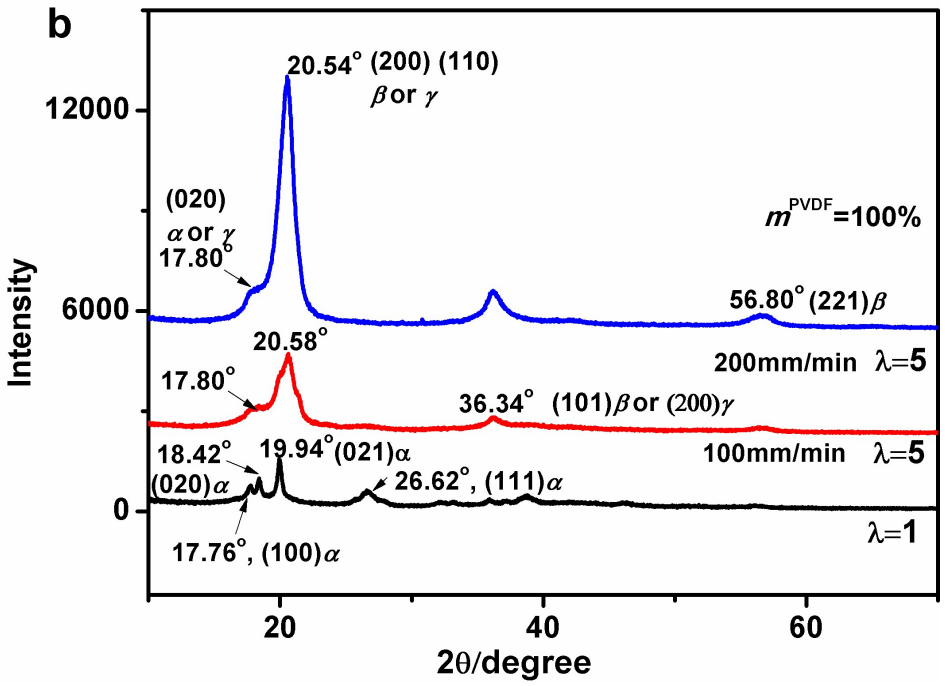
b
20.54° (200) (110)
β or γ
(020)
α or γ
17.80°
m^PVDF=100%
56.80° (221)β
20.58°
200mm/min λ=5
17.80°
36.34° (101)β or (200)γ
18.42°
19.94°(021)α
100mm/min λ=5
(020)α
26.62°, (111)α
λ=1
17.76°, (100)α
Intensity
2θ/degree

Fig. 9

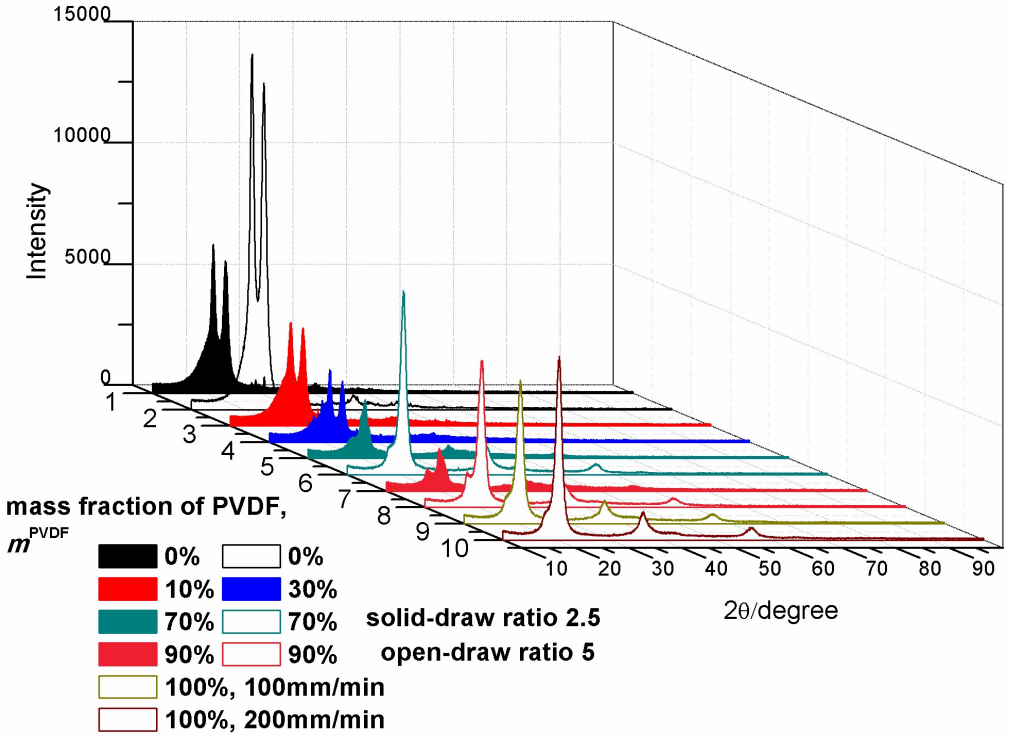
Intensity
2θ/degree
mass fraction of PVDF,
m^PVDF
0%
0%
10%
30%
70%
70%
90%
90%
100%, 100mm/min
100%, 200mm/min
solid-draw ratio 2.5
open-draw ratio 5

Fig. 10